ELSEVIER

Journal of Nuclear Materials 241–243 (1997) 956–960

journal of nuclear materials

Behavior of pellet injected Li into Heliotron E plasmas

K. Kondo [a,*], K. Ida [c], C. Christou [a], V.Yu. Sergeev [d], K.V. Khlopenkov [d], S. Sudo [c], F. Sano [b], H. Zushi [a], T. Mizuuchi [b], S. Besshou [a], H. Okada [b], K. Nagasaki [b], K. Sakamoto [b], Y. Kurimoto [e], H. Funaba [e], T. Hamada [e], T. Kinoshita [e], S. Kado [f], Y. Kanda [e], T. Okamoto [e], M. Wakatani [a], T. Obiki [b]

[a] *Graduate School of Energy Science, Kyoto University, Uji, Japan*
[b] *Institute of Advanced Energy, Kyoto University, Uji, Japan*
[c] *National Institute for Fusion Science, Nagoya, Japan*
[d] *St. Petersburg Technical University, St. Petersburg, Russia*
[e] *Faculty of Engineering, Kyoto University, Kyoto, Japan*
[f] *Interdisciplinary Graduate School of Engineering Science, Kyushu University, Kasuga, Japan*

Abstract

Li pellet injection has provided a complex plasma with a large fraction of Li ions, which is characterized by intense emissions from Li I and III. The spatial profiles of the fully ionized Li^{3+} ions are measured by charge exchange recombination spectroscopy with a resolution of 13 mm and the local decay time of the injected Li ion has been estimated. The spectral profile of the charge exchange recombination line of Li III from $n = 5$ to $n = 4$ shows a complicated structure, which depends on Li^{3+} density. The effects on other intrinsic impurities and recycled Li are also discussed.

Keywords: Heliotron E; Stellarator; Impurity transport; Line emission diagnostic; Wall conditioning

1. Introduction

Li pellet injection has been recently in producing high performance plasmas [1–3]. The ablation mechanism of a Li pellet is also of interest because of the high sublimation energy compared to hydrogen and deuterium pellets [4,5]. The development of Li pellet injectors and study of the interaction between injected Li atoms and the plasma are thus urgent issues for fusion oriented experiments. For Heliotron E [6], a Li-pellet injector has been developed in order to obtain good performance plasmas, to study the ablation mechanisms and to establish a new diagnostic method for the measurement of the magnetic field direction. The injected Li is also used as a tracer for investigating particle transport and for analyzing spectral profiles of Li ions.

In this paper, the behavior of Li atoms and ions injected in neutral beam heated plasmas is stated. In particular fully ionized Li^{3+} ions are measured by a charge exchange recombination spectroscopy and the local decay time of Li^{3+} is estimated. Effects of deposited Li on the inner surfaces of the vacuum chamber on hydrogen recycling and oxygen impurity are also described.

2. Li pellet injector and diagnostics

The Li pellet injector consists of a magazine for pellets, gun barrel, guide tubes and differential pumping system with a buffer tank of 0.1 m^3 [7]. 30 pre-shaped Li pellets 1 mm in diameter and length are filled into the holes in the rotatable disk of the magazine. A single pellet has 3.6×10^{19} Li atoms. The gun barrel is 1 m long and 1 mm in diameter. The four guides are 0.14, 1.5, 0.4 and 2.7 m long, the diameters are 2.27, 4, 7.53 and 10.7 mm, respectively. High pressure He is used as a propellant gas. The

* Corresponding author.

PII S0022-3115(96)00640-X

injection speed is 400–500 m/s, which is measured between the gun barrel and the first guide tube. The pellet trajectory distributes within a cone of 1° full angle. Pellets are injected horizontally and cross the plasma column nearly perpendicularly. The minor radius of the plasma column is 0.3 m and the ablation time is 1.2 ms. A high speed camera is used to record images of the ablation cloud at every 50 μs. Two optical filters for Li I (6706 Å) and Li II (5485 Å) are provided to estimate the ablation rates. A multi-channel vacuum ultraviolet spectrometer, which is available from 45 to 400 Å, is used to measure Li III (135 Å) emission. The neutral Li I (6706 Å) emitted near the wall is measured by a visible spectrometer, which is located at 132° in the toroidal direction from the port of the pellet injector. A 1.26 m visible spectrometer with a 2D detector (Hamamatsu, C3554X) [8] is employed to analyze the spectral profiles of the Li^{2+} line populated by charge exchange recombination from Li^{3+} ion. The time resolution is 20 ms. The sight-lines of 40 fiber optics cross the plasma column from 1.98 to 2.42 m on a major radius and the spatial resolution is 13 mm. The profiles of the electron density and temperature are measured by a Thomson scattering system [9] and ion temperature profile is estimated by the charge exchange recombination line of C VI.

3. Behavior of Li ions

An Li pellet is injected into a plasma, which is initiated by a 106 GHz gyrotron and further heated by neutral beams of 3.5 MW power. The acceleration voltage of the neutral beams is 23 kV. The magnetic field strength is 1.9 T. The vacuum chamber wall has been 'boronized' by using an ECH discharge with $B_{10}H_{14}$ and He [10]. Fig. 1 shows the time evolutions of the average electron density with and without Li pellet injection. The incremental electron density due to the pellet injection is also shown. The

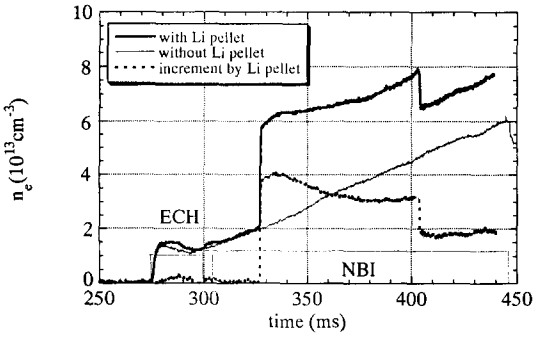

Fig. 1. The time evolutions of the average electron densities. The solid line is for the shot with Li pellet injection at 336 ms and the dotted line corresponds to the shot without pellet injection. The incremental electron density due to the pellet injection is also plotted.

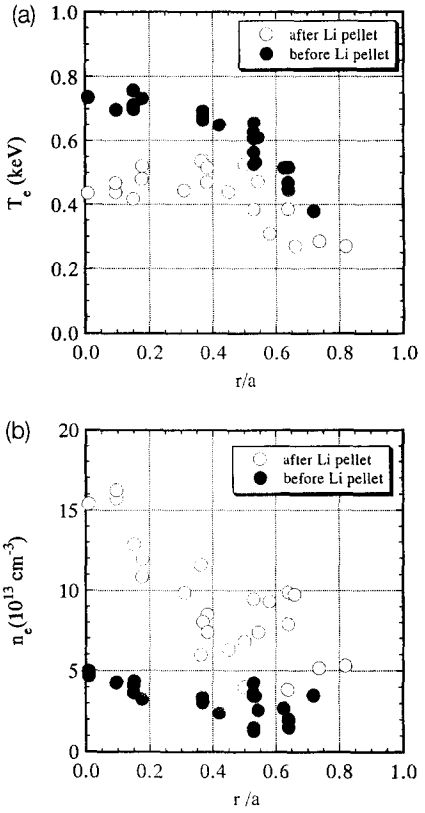

Fig. 2. The electron temperature (a) and density (b) profiles immediately before (closed) and 4–6 ms after (open) the pellet injection.

plasma is produced at 275 ms and the neutral beam heating starts at 300 ms and terminates at 444 ms. After the Li pellet is injected at 327 ms, the average electron density increases by 4×10^{13} cm^{-3}. Fig. 2(a), (b) show the profiles of the electron temperature and density immediately before and 4–6 ms after the Li pellet injection measured by Thomson scattering. The central electron temperature drops from 0.75 to 0.45 keV and the central electron density increases from 4.5×10^{13} cm^{-3} to 1.4×10^{14} cm^{-3}. The electron energy has almost doubled after the Li pellet injection. The ablation rate of 3.5×10^{22} atoms/s is estimated at the plasma center. In this case, the increase of the electron density is smaller than that provided by the entire Li pellet because the injected Li pellet does not completely ablate. About 60% of the pellet is deposited in the plasma. The density ratio of the Li^{3+} ions to protons is estimated to be 0.6, but this ratio decreases rapidly as shown later.

Fig. 3 shows spectra in the wavelength region from 170 to 400 Å before (320 ms) and after (330 ms) the Li pellet injection. The integration time is 10 ms. The base line is shifted in the upper spectrum. The prominent line is Li III (135 Å), which appears at 270 Å in second order. The

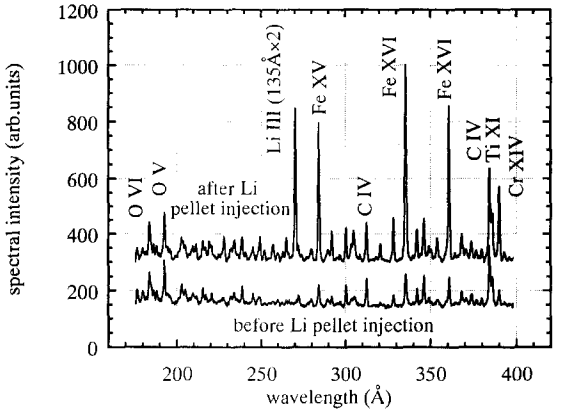

Fig. 3. The spectra in the vacuum ultraviolet region before and after the pellet injection. Li III (135 Å) appears at 270 Å in second order. Time resolution is 10 ms.

emission of Li II (199.3 Å) is not observed. Other prominent lines originate from intrinsic impurities such as carbon, oxygen, titanium, chromium and iron. Fig. 4 shows the time evolution of the Li III. O V (192.9 Å) and Fe XV (284.1 Å) emissions are also shown as typical examples of light and heavy impurities. Immediately after Li pellet injection emission of Li III peaks and decreases with a decay time of about 60 ms. Similarly a sharp peak appears in Fe XV emission, which increases again at 360 ms up to the end of the neutral beam pulse due to continuous influx of iron. The pellet injection causes emission from the high ionization states of metallic impurities to increase significantly but appears to have a much smaller effect on oxygen and carbon emission. This suggests that the pellet penetrates into the plasma core and iron emission may be enhanced by either an increase in central electron density or by recombination of higher ionization states caused by a drop of the electron temperature.

The fully ionized Li^{3+} ion has been studied using charge exchange recombination spectroscopy. The transition from $n = 5$ to $n = 4$ is used, with a wavelength of 4499 Å [11]. Fig. 5 shows the intensity profiles of 4499 Å

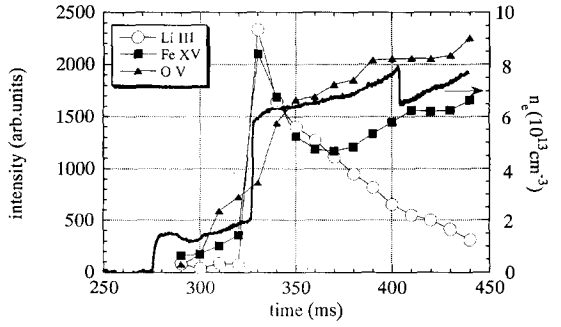

Fig. 4. The time evolutions of the intensities of Li III, O V and Fe XV.

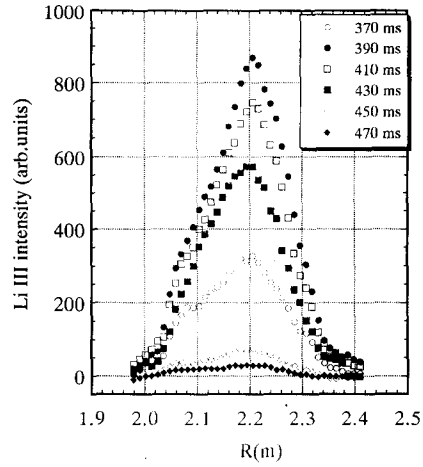

Fig. 5. Spatial profiles of Li III emissions measured by charge exchange recombination spectroscopy. The Li pellet is injected at 378 ms. Time resolution is 20 ms.

from 370 ms to 450 ms. The horizontal axis is the major radius and the magnetic axis is located at 2.2 m. The Li pellet is injected at 378 ms. The decay time of Li^{3+} is estimated at various locations by exponential filling from 390 ms to 430 ms. At $R = 2.2$ m, on the magnetic axis, the decay time is 90 ms and 160 ms is obtained at $R = 2.1$ m and 60 ms at $R = 2.3$ m. There appears an asymmetry between inboard and outboard of the plasma column. This asymmetry is attributed to the slow increase of the penetrated neutral beam density in the inboard due to the decrease in the electron density as described later. The Li III (135 Å), observed by the VUV spectrometer, shows a decrease with a decay time of 60 ms. In this shot the

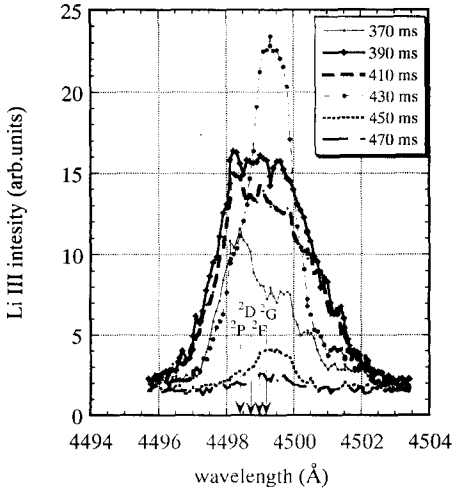

Fig. 6. Spectral profiles of Li III charge exchange recombination line from $n = 5$ to $n = 4$ transition. Arrows indicate the calculated average wavelengths from designated upper levels.

average electron density increased from 2.5×10^{13} cm^{-3} to 9×10^{13} cm^{-3} by the pellet and then decreased to 7×10^{13} cm^{-3} with a decay time of 160 ms.

Fig. 6 shows the spectral profiles of around 4499 Å at successive times after the pellet. There appear to be several line components, which are in the wavelength region corresponding to transitions from the $n = 5$ sublevels; ^{2}P, ^{2}D, ^{2}F and ^{2}G. Arrows in the figure indicate the calculated average wavelengths from designated upper levels. The shorter wavelength components are dominant in the early phase after the Li injection. As Li density decreases, the dominant component shifts to the longer wavelength. This corresponds to the transition from low orbital angular momentum to high orbital angular momentum transitions. The depopulation among the levels due to collision in high density regime is considered as a candidate for the explanation, but there is no similar phenomenon in carbon. In the Li^{3+} ion case, the density is so large it is possible that this depopulation is due to collisions among Li ions.

4. Behavior of the neutral Li line

It is an important issue to investigate the effects of the Li pellet injection on hydrogen recycling and the behavior of intrinsic impurity. To analyze above problems it is necessary to measure shot-to-shot variations of Li, electron density and impurity. Neutral Li emission at 6706 Å is used to study the behavior of recycled Li after the Li pellet injection. The observation port is located by 132° from the pellet injection port. A spectrometer with a focal length of 1.26 m and a 1024-channel diode array detector is used. The time resolution is 10 ms. Fig. 7 shows the time evolutions of the Li I intensities in successive shots with and without Li pellet injection. As Li pellet is injected, a large increase in Li I intensity is observed. This means that the injected Li is transported all around the torus. In the next shot (#71113), the Li I intensity increases than before shot in 300–370 ms, which indicates the Li is deposited on the inner surfaces of the vacuum vessel. Fig. 8 shows the

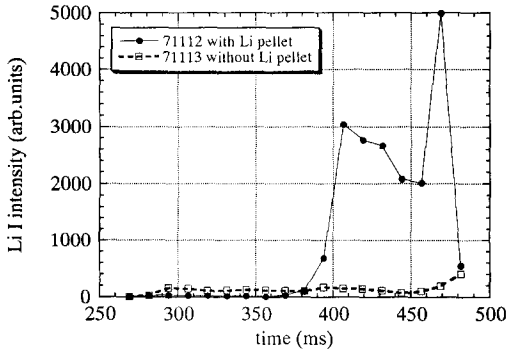

Fig. 7. Time behavior of Li I intensity in successive shots with and without the Li pellet injection.

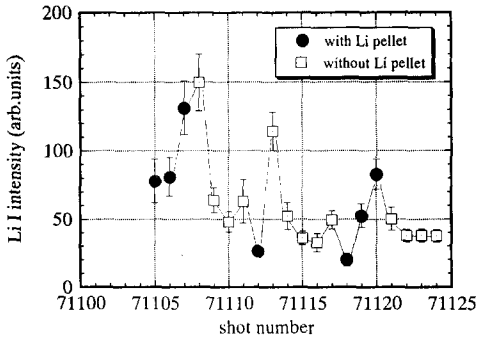

Fig. 8. Li I intensity at 300–360 ms in successive shots with and without Li pellets. Closed circles are with the Li pellet injection at 378 ms and open squares are without.

shot-to-shot variations of Li I intensity. Li pellet shots are denoted by closed circles and open squares correspond to shots without a pellet. The Li I intensities are estimated from 330 to 370 ms. In these shots the neutral beam of 3.2–3.4 MW power is injected from 300 to 440 ms. For the pellet shots Li pellet is injected at 378 ms. The Li I emission is again visible from shots following pellet injection shots indicating Li recycling. Injection of Li pellets in successive shots can cause a cumulative increase in Li I emission and a gradual fall in Li I emission can be seen one to two shots after Li pellet injection has ceased. From the density increase the deposited Li is estimated as 3×10^{19} atoms/shot. Then the deposited Li layer is estimated to be less than one monolayer if Li spreads uniformly on all internal surfaces of the vacuum vessel (3×10^5 cm^2). The average electron density for the shot #71105 is 1.1×10^{13} cm^{-3} at 300 ms and increases to 3.9×10^{13} cm^{-3} at 360 ms immediately before Li pellet injection. The increasing rate of the electron density decreased from 4.6×10^{14} cm^{-3} s^{-1} at #71105 to 1.6×10^{14} cm^{-3} s^{-1} at #71124. The reduction in hydrogen recycling has been observed by Li pellet injection. Behavior of oxygen impurity is an interesting issue for the Li pellet injected shots. O V emission at 629 Å is measured by a vacuum ultraviolet

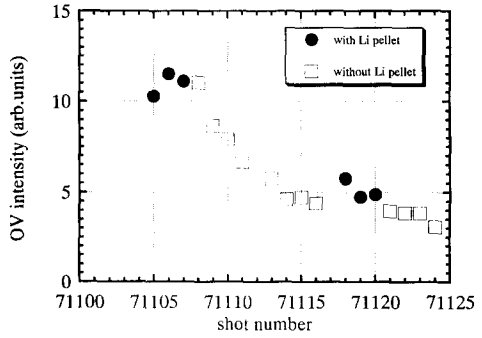

Fig. 9. O V intensity at 350 ms in successive shots with and without Li pellets. Closed circles are with the Li pellet injection at 378 ms and open squares are without.

spectrometer with a focal length of 2.2 m. The intensity at 300 ms decreases monotonously in contrast to Li I by about 1/2 in these 20 shots as shown in Fig. 9.

5. Conclusion

In Heliotron E, a Li pellet injector with good reproducibility and reliability has been developed and successfully injected into neutral beam heated plasmas. The spatial profiles of Li III emission from Li^{3+} are measured with a spatial resolution of 13 mm and local decay time is estimated. This diagnostic method can be used to estimate the local values of diffusion coefficient for impurities. As Li has low ionization energy, fully ionized Li^{3+} distributes from the core to the edge of the plasma column and this is very convenient to analyze impurity transport phenomena. Moreover the emission intensity is determined only by the product of neutral beam and Li^{3+} densities so complicated analysis on excitation and ionization is not necessary. The fine structure from sublevels of the charge exchange recombination line from $n = 5$ to $n = 4$ is analyzed. The collision among Li ions is considered to be the most probable candidate for the depopulation. From the measurements of the neutral Li I emission, the injected Li is transported all around the torus and deposited on the inner surfaces of the vacuum chamber. The persisted Li remains one or two shots after the Li injected shots and the thickness of the deposited Li is estimated to be one monolayer. However it is effective to reduce the hydrogen recycling and oxygen impurity.

Acknowledgements

The authors are grateful to the Heliotron group for their excellent and helpful support. The authors would like to thank Dr. J. Terry for critical reading of the manuscript.

References

[1] J.L. Terry et al., 13th IAEA, Washington, Vol. 1 (1990) 393.
[2] J.A. Snipes, E.S. Marmar, J.L. Terry et al., J. Nucl. Mater. 196–198 (1992) 686.
[3] D.K. Mansfield et al., Phys. Plasmas 2 (1995) 4252.
[4] B.V. Kuteev, V.Yu. Sergeev and L.D. Tsendin, Sov. J. Plasma Phys. 10 (1984) 675.
[5] P.B. Parks, J.S. Leffler and R.K. Fisher, Nucl. Fusion 28 (1988) 477.
[6] T. Obiki et al., 15th Int. Conf. on Plasma Physics and Controlled Nuclear Fusion Research, Seville, 1994, Vol. 1 (IAEA, Vienna, 1995) p. 757.
[7] K.V. Khlopenkov, V.Yu. Sergeev, S. Sudo et al., 7th Int. Conf. on Plasma Physics and Controlled Nuclear Fusion, Toki, Japan (1995).
[8] K. Ida and S. Hidekuma, Rev. Sci. Instrum. 60 (1989) 867.
[9] H. Funaba, H. Okada et al., 7th Int. Conf. on Plasma Physics and Controlled Nuclear Fusion, Toki, Japan (1995).
[10] K. Kondo, T. Mizuuchi et al., J. Nucl. Mater. 220–222 (1995) 1052.
[11] S. Bashkin and J.O. Stoner, Atomic Energy Levels and Grotrian Diagrams, Vol. I (North-Holland, Amsterdam, 1975).